Tenofovir-silver nanoparticles conjugate ameliorates neurocognitive disorders and protects ultrastructural and cytoarchitectonic properties of the prefrontal cortex in diabetic rats

Sodiq Kolawole Lawal[1]*, Samuel Oluwaseun Olojede[1], Sheu Oluwadare Sulaiman[2], Okikioluwa Stephen Aladeyelu[1], Roshila Moodley[3], Edwin C. Stephen Naidu[1], Carmen Olivia Rennie[1], Onyemaechi Okpara Azu[4]

ABSTRACT

Tenofovir disoproxil fumarate (TDF) is the highly recommended antiretroviral drug in human immunodeficiency virus management. Although research has shown the neurological and metabolic disorders associated with TDF administration, the effect of TDF-silver nanoparticles conjugate (TDF-AgNPs) on the disorders has not been fully elucidated. Thus, this study evaluated the neuroprotective effects of TDF-AgNPs on ultrastructural and cytoarchitectonic properties of the prefrontal cortex (PFC) in diabetic rats. Forty-two adult male Sprague-Dawley rats (250 ± 13 g) were randomly divided into non-diabetic groups (1–3) and diabetic groups (4–6), each administered distilled water (0.5 ml/100g, p.o), TDF (26.8 mg/kg/bw, p.o) or TDF-AgNPs (6.7 mg/kg, i.p). After eight weeks of administration, cognitive function, oxidative injury, and tissue inflammation were evaluated. Furthermore, PFC ultrastructure was observed using transmission electron microscopy, Nissl staining, and immunohistochemistry. Diabetic rats administered TDF exhibited cognitive deficits; and increases in blood glucose, malondialdehyde, and interleukin-1 beta (IL-1β) levels, which correlate with decreases in glutathione level, and superoxide dismutase (SOD) and catalase (CAT) activities. Furthermore, loss of PFC astrocytes and neuronal organelles was observed. Conversely, TDF-AgNPs administration to diabetic rats improved cognitive deficits; and increased glutathione, SOD, and CAT, but reduced PFC malondialdehyde and IL-1β concentrations. Notably, TDF-AgNPs prevented loss of PFC neurons and astrocytic cells, and morphology aberration of neuronal organelles. This study suggests that TDF-AgNPs attenuated cognitive deficits via silver nanoparticles' antioxidant and anti-inflammatory properties, preventing the loss of PFC astrocytes and neurons. The TDF-AgNPs may be utilized to ameliorate the neurological dysfunction caused by prolonged TDF administration.

KEYWORDS: Tenofovir; prefrontal cortex; silver nanoparticles; neuroinflammation; neurological dysfunction

[1]Discipline of Clinical Anatomy, School of Laboratory Medicine and Medical Sciences, Nelson R Mandela School of Medicine, University of KwaZulu-Natal, Durban, South Africa
[2]Postgraduate Program in Cell Biology and Birbrair Laboratory, Institute of Biological Sciences, Federal University of Minas Gerais (UFMG), Minas Gerais, Belo Horizonte, Brazil
[3]School of Chemistry and Physics, University of KwaZulu-Natal, Westville Campus, Durban, South Africa
[4]Department of Anatomy, School of Medicine, University of Namibia, Windhoek, Private, Namibia

*Corresponding author: Sodiq Kolawole Lawal, Discipline of Clinical Anatomy, School of Laboratory Medicine and Medical Sciences, University of KwaZulu-Natal, Private Bag X 54001, Durban 4000, South Africa. E-mail: lawalsodiq6@gmail.com, 219083228@stu.ukzn.ac.za

INTRODUCTION

The introduction of combined antiretroviral therapy (cART) has a tremendous positive impact in managing patients living with the human immunodeficiency virus (HIV) [1,2]. The cART has multiple benefits, such as suppressing HIV replication, reducing HIV to a manageable level, and improving the quality of life among HIV-positive people [3-5].

Despite the benefits of cART, prolonged usage has been associated with oxidative stress, neuronal injury, and mitochondrial dysfunction leading to neurological and cognitive deficits [6,7].

The standard cART, as a fixed dose, consists of two nucleoside reverse transcriptase inhibitors (NRTIs) with either one of the non-nucleoside reverse transcriptase inhibitors, protease inhibitors, or integrase inhibitors [8]. The NRTIs such as Tenofovir disoproxil fumarate (TDF), emtricitabine, and lamivudine are considered the backbone of cART due to their antiviral efficacy and narrower

resistance barrier [9]. TDF is the most recommended NRTIs used in HIV pre-exposure or post-exposure prophylaxis. However, TDF is ranked as a low central nervous system (CNS)-penetration drug considering its physicochemical characteristics, cerebrospinal fluid concentration, and effectiveness in the CNS [9-11]. More so, a 25% reduction in the TDF concentration was observed in dried blood spots of people with diabetes mellitus compared with non-diabetic control (NC) adults [12]. Besides, long-term administration of NRTIs, especially TDF, is associated with metabolic disorders, diabetes mellitus, and systemic and organ toxicity [13,14]. Insulin-like growth factor-1 (IGF-1) is involved in the pathogenesis of metabolic disorders related to diabetes and its complications [15]. Studies have reported the negative impact of TDF on the IGF-1 level in blood and brain samples and its implication in diabetes [16,17].

Furthermore, NRTIs need intracellular anabolic phosphorylation in the host cell to form phosphorylated NRTI metabolites, which have been associated with mitochondrial toxicity and oxidative injury [18,19]. Oxidative neuronal injury, mitochondrial dysfunction, and neuroinflammation have been implicated in neurocognitive deficits [20,21]. The prefrontal cortex (PFC) plays a vital role in cognitive and executive functions, and it is an established brain area to study working memory in animal models [22-24]. Studies have reported that ultrastructural brain injury and up-regulated inflammatory cytokines (e.g., interleukine-1 beta [IL-1β]) were associated with cognitive dysfunction in HIV-positive children on long-term cART [11,25].

Despite the benefits of TDF in HIV management and control, studies have proposed its dose modification in people living with diabetes mellitus and HIV due to its low CNS penetration and neurotoxicity [11,12]. For these reasons, using the nano-delivery system to navigate TDF via the bloodbrain barrier and improving its CNS concentration while minimizing its neurotoxic effects would provide immense therapeutic benefits. Nanoparticles hold promise in delivering antiretroviral drugs due to their ability to cross the biological barrier and long-term release while achieving drug efficacy [26-28]. Silver nanoparticles (AgNPs) are known for their unique properties such as morphology, size, and high surface to volume ratio, making them suitable to be used as intracellular delivery agents [29]. Silver nanoparticles are the most widely used nanoparticles in biomedical sciences as antioxidant and antidiabetic agents [30-32], which may reduce the metabolic and neurotoxic effects of TDF.

Hence, this study aimed at evaluating the therapeutic and neuroprotective effects of Tenofovir-silver nanoparticles conjugate on the cognitive function, and ultrastructural and cytoarchitectonic properties of the PFC in experimental type-2 diabetic rats.

MATERIALS AND METHODS

Drugs and chemicals

Enzyme-linked immunosorbent assay (ELISA) kits for IL-1β (Cat No. E-EL-R0012) and IGF-1 (Cat No. E-EL-R0010) were purchased from BIOCOM Africa (pty), Ltd, (South Africa). Streptozotocin (STZ), trisodium citrate (TSC), sodium hydroxide, and silver nitrate ($AgNO_3$) were purchased from Sigma-Aldrich (South Africa). Moreover, TDF (TDF, 300 mg) was purchased from Dis-Chem pharmacy Durban, South Africa.

Experimental animals

Forty-two adult male Sprague-Dawley rats (250 ± 13 g) were obtained from the University of KwaZulu-Natal, Biomedical Research Unit (BRU). The rats were housed in the standard animal laboratory room, maintained at a temperature of 24-26° C, 12:12 light: dark cycle and 40-60% humidity.

Experimental design

After acclimatization for 7 days, the rats were randomly divided into six groups (n = 7/group) and treated for eight weeks. Groups 1-3 were non-diabetic rats designated as NC administered 0.5 ml/100g distilled water per os (p.o.), non-diabetic + Tenofovir (NT) administered 26.8 mg/kg/bw TDF p.o., and non-diabetic + silver-nanoparticles + tenofovir (NST) administered 6.7 mg/kg TDF-AgNPs intraperitoneally (i.p.). Groups 4-6 were diabetic rats designated as diabetic control (DC) administered 0.5 ml/100g distilled water p.o., diabetic + Tenofovir (DT) administered 26.8 mg/kg/bw TDF p.o., and diabetic + silver-nanoparticles + tenofovir (DST) administered 6.7 mg/kg TDF-AgNPs i.p. The drug dosage was determined according to Everson et al. [33].

Induction of type 2 diabetes mellitus in rats

Type 2 diabetes mellitus was induced using the fructose-STZ rat model as described by [34]. Briefly, Groups 4-6 rats received 10% fructose solution *ad libitum* for two weeks. On the last day of fructose administration, the rats were fasted overnight, followed by a single intraperitoneal injection of freshly prepared 40 mg/Kgbw STZ dissolved in 0.9% NaCl with 100 mM sodium citrate buffer (pH 4.5) [35]. The control rats received an equal volume of vehicle (citrate buffer). Animals with fasting blood glucose (BG) levels ≥200 mg/dL were considered diabetic and included in this study.

Formulation of TDF silver nanoparticles (TDF-AgNPs)

Silver nanoparticles (AgNPs) were synthesized according to the method of Turkevich et al. [36]. Briefly, silver nitrate

($AgNO_3$) crystals were oven-dried at 100° C. Then, 0.3 g of the $AgNO_3$ was weighed into a 500 ml volumetric flask and dissolved with double distilled water to prepare an aqueous solution (0.03 M). The aqueous stock solutions (0.5M, 1M, 1.5M, and 2M) of TSC were prepared from 14.7 g, 29.41 g, 44.12 g, and 58.82 g of TSC in 250 mL of double-distilled water and used as reducing and stabilizing agent. The resultant solution of each of the four different TSC concentrations and $AgNO_3$ was continuously stirred for 5 minutes at 90° C, adjusted to pH 10.5 using sodium hydroxide (NaOH), and then stirred for 90 minutes at 90 °C during which color changes were observed from colorless to amber yellow. The synthesized silver nanoparticles (AgNPs) were cooled at room temperature, centrifuged at 12 000 rpm for 15 minutes, and then oven-dried at 40° C for 12 hours.

The TDF silver nanoparticles (TDF-AgNPs) were synthesized by mixing 100 ml of different concentrations (0.5 M, 1 M, 1.5 M, 2 M) of synthesized AgNPs with a 100 ml stock solution of TDF (0.35 M). The final mixture (TDF-AgNPs) was stirred on an ultra-sonicator to ensure proper reaction of TDF and AgNPs. After that, TDF-AgNPs were centrifuged at 4,500 rpm and 40° C, for 40 minutes. The supernatant obtained was analyzed with a UV spectrophotometer at a wavelength of 364 nm to calculate the percentage incorporated efficiency.

TDF-AgNPs percentage incorporated efficiency (% IE) was calculated according to the method of Govender et al. [37] as

$$\% \, IE = \frac{w_2 - w_1}{w_1} \times 100 \quad = 85.00 \pm 0.0 \, \%.$$

W_1 = quantity of unincorporated drug and W_2 = total amount of drug coupled with the silver nanoparticles.

The characterization of AgNPs and TDF-AgNPs was done to select the appropriate TSC concentration based on the nanoparticles' absorbance peaks, size and shape, and morphology of the conjugated TDF-AgNPs. The ultraviolet-visible (UV-Vis) spectroscopy (Shimadzu MultSpec-1501, Shimadzu Corporation, Tokyo, Japan) indicated an absorption peak from 325 to 328 nm. Fourier transform infrared spectroscopy (Perkin-Elmer Universal ATR spectrometer, USA) was used to identify the various functional groups in the TDF-AgNPs conjugates. The functional groups C-N and O-H were present on TDF-AgNPs, indicating that TDF was successfully incorporated into AgNPs.

Furthermore, the high-resolution transmission electron microscope (HR-TEM, JEOL 2100, Japan) operated at a voltage of 200 kV showed spherical particles for 2 M of TDF-AgNPs, and the particle size was between 12 nm and 22 nm.

The field emission scanning electron microscope (FESEM, Carl Zeiss, Germany) operated at a voltage of 5 kV with energy dispersive X-ray (EDX, Aztec Analysis Software, England), and the EDX was used to determine the elemental components. This analysis revealed the presence of silver, sodium, and other functional groups from AgNPs and TDF, indicating that the silver nanoparticles were successfully incorporated with TDF.

Blood glucose (BG) level

The blood samples were obtained through the tail vein, and the BG measurement was determined using a portable glucometer (Sigma-Aldrich, Durban, South Africa).

Behavioral assessment

The Y maze test was used to measure the experimental rats' cognitive functions (working memory) and explorative behaviors. The "spontaneous alternation performance" and "same arm return (SAR)" was done following previously used methods [38,39]. Briefly, Y-maze comprises three equal arms, each measuring 40 cm long, 15 cm high, and 10 cm wide, and interconnected with one another at 120°. The arms were identified as A, B, and C. Each rat started the experiment at the center of the maze and was allowed to move freely for 5 minutes. The whole body must completely enter the arm from the center area before recording is taken as one entry. The number of entries was recorded using a video camera, and two independent observers recorded the data from the computer system.

Spontaneous Alternative Performance (SAP) and SAR were analyzed, and the percentage alternation was calculated as previously reported [39]:

% Alternation = (Number of Alternations/[Total number of arm entries-2]) × 100).

Neurochemical analysis

Preparation of brain homogenates

The brain tissue was harvested and immediately rinsed in cold phosphate-buffered saline (PBS), and the PFC was dissected on the ice tray. PFC (0.5 g) was weighed and homogenized in 5 mL of sodium phosphate buffer (0.1M, pH 7.5). The homogenates were centrifuged for 10 mins at 20,000 g, and the supernatants were obtained for neurochemical analyses.

Determination of superoxide dismutase (SOD) and catalase (CAT) activities, and reduced glutathione (GSH) and malondialdehyde (MDA) levels

PFC tissue homogenates were analyzed for SOD and CAT activities as well as GSH and MDA levels by spectrophotometric assay. SOD and CAT activities were determined following the methods of Kakkar et al. [40] and Aebi [41], respectively. Reduced GSH level was assessed using the Ellman protocol [42]. MDA level was determined by measuring the content of thiobarbituric acid reactive products using the method of Mkhwanazi et al. [43].

Analysis of inflammatory biomarkers

The concentrations of cytokine IL-1β and IGF-1 were quantified in the PFC homogenates using their specific ELISA

kits (Elabscience Biotechnology Co., Ltd., Houston, TX, USA) according to the manufacturer's instructions.

Brain tissue processing for microscopic study

The brains were carefully removed from the rat's skull and then postfixed in 10% neutral buffer formalin (NBF) for 1 hour. It was then transferred to 15% sucrose in PBS (24 hours) followed by 30% sucrose in PBS for 12 hours and finally fixed in 10% NBF for histology and immunochemistry through paraffin embedding. The PFC tissues were sectioned at 5 μm using Leica RM 2255 microtome, followed by clearing in xylene, hydration in descending grades of alcohol, Nissl staining according to [44], and mounting with dibutyl phthalate polystyrene xylene [45].

Immunohistochemical (IHC) analysis

The PFC was used for the IHC analysis of Glial Fibrillary Acidic Protein (GFAP). The sections were washed in PBS 2 times for 10 minutes each (2 × 10 minutes) at 4° C and pre-incubated in 0.1 M PBS. This process was followed by 5% normal goat serum with 0.4% Triton X-100 and 1% bovine serum albumin for one hour at 4° C. The process was then followed by a direct incubation in the GFAP primary antibody (anti-GFAP) diluted in the phosphate-buffered Sodium Azide (PBSA)-Triton (PBSAT). After that, tissue sections were incubated in 0.1 M PBS containing 2% normal goat serum and biotinylated rabbit anti-goat IgG (secondary antibody) (1:2000) for 2 hours at room temperature. The sections were then rinsed in PBSAT (2 × 10 minutes) and then incubated with the avidin-biotin complex (AB; 1:2000) for 2 hours at room temperature, followed by several washes (1 × 10 minutes in PBST and 2 × 10 minutes in Tris buffer [0.05 M, PH 7.6]). The peroxidase activity detection was carried out with 3-3' diaminobenzidine (DAB, 0.025%, 0.5% Nickel ammonium sulphate in tris buffer (0.1 M, pH 7.6) with 0.03% hydrogen peroxide. After that, the immunoreactive reaction was stopped by washing the sections once in 0.1 M Tris buffer (10 minutes) and then twice in 0.1 M PBS (10 minutes). Sections were dehydrated in ascending grades of ethanol baths, cleared in two successive xylene baths, mounted onto gelatin-coated slides, and covered slipped with Eukitt.

Ultrastructural tissue processing

The brain tissues were initially fixed in buffered 2.5 % glutaraldehyde for 12 hours, washed in phosphate buffer (3 × 5 minutes), and postfixed in 1 % osmium tetroxide for 2 hours. This was followed by washing in phosphate buffer (3 × 5 minutes), dehydrating in ascending grades of Acetone (30%, 50%, 75%, and 100%) for 5 minutes each, and embedding in Durcopan

(Fluka). Ultrathin sections of PFC were cut using an ultramicrotome, contrasted by uranyl acetate and lead acetate, and the prepared tissue sections were examined by transmission electron microscopy (TEM).

Ethical statement

All rats were handled following standard guides for the animal laboratory and were allowed free access to water and feed *ad libitum*. The experimental protocols were approved by the Animal Ethics Committee (AREC) of the University of KwaZulu-Natal (AREC/044/019D).

Statistical analysis

Data were presented as mean ± SEM. The differences between means were compared using one-way analysis Analysis of variance, followed by Tukey's multiple comparisons test. All analyses were done using GraphPad Prism 8 for Windows (GraphPad Software San Diego, CA 92108). $p < 0.05$ was considered statistically significant.

RESULTS

TDF-AgNPs reduces BG and PFC IGF-1 levels

The results in Table 1 show that there was a significant ($p < 0.05$) increase in BG level in the DC group (DC) compared with the non-diabetic group (NC). In non-diabetic groups, there was an increased BG level in TDF treated group (NT) (89.26 ± 26) compared with NC (80.86 ± 2.65). Notably, the non-diabetic group treated with TDF-AgNPs (74.26 ± 1.52) had a significant reduction ($p < 0.05$) in the BG compared with TDF treated only.

Diabetic rats treated with TDF (group DT) (416.9 ± 19.26) had a significant increase ($p < 0.05$) in BG level compared with DC (334.0 ± 8.6). Interestingly, the rats administered with TDF-AgNPs (DST) (279.4 ± 12.17) had a significant decrease ($p < 0.05$) in BG level compared with DC and diabetic + TDF group (DT).

TABLE 1. Blood glucose and prefrontal cortex Insulin-like growth factor-1 levels

Groups	BG (mg/dl)	IGF-1 (ng/g)
Group 1 (NC)	80.86±2.650	1378±56.72
Group 2 (NT)	89.29±2.495	1268±107.3
Group 3 (NST)	74.29±1.523*	1376±74.44
Group 4 (DC)	334.0±8.555[a]	376.2±20.12 [a]
Group 5 (DT)	416.9±19.26[b]	263.3±10.22[b]
Group 6 (DST)	279.4±12.17[bc]	562.5±36.22[bc]

[a]$p<0.05$ versus NC, [b]$p<0.05$ versus DC, [c]$p<0.05$ versus DT.
*$p<0.05$ versus NT. NC=nondiabetic control, NT=non-diabetic+TDF, NST=non-diabetic+silver nanoparticles+TDF, DC=diabetic control, DT=diabetic+TDF, DST=Diabetic+silver nanoparticles+TDF. Data are presented as mean±SEM and are significant at $P<0.05$

In non-diabetic groups, TDF-treated group NT (1268 ± 107.3) had a decrease in IGF-1 compared with NC rats (NC) (1378 ± 56.72) and group NST (TDF-AgNPs) (1376 ± 74.44). The DC group (DC) (376.2 ± 20.12) had a significant ($p < 0.05$) decrease in IGF-1 compared to the NC group (NC). IGF-1 was significantly decreased in group DT (diabetic + TDF) (263.3 ± 10.22) compared with group DC. However, group DST (diabetic + AgNPs+ TDF) (562.5 ± 36.22) had a significant increase in IGF-1 compared with group DC and group DT.

TDF-AgNPs improves cognitive functions using Y-maze

As shown in Table 2, there was a significant decrease in spontaneous alternation performance (a measure of cognitive performance) and an increase in SAR in all diabetic groups (DC, DT, and DST) compared with NC. Furthermore, there was a significant decrease in SAP in diabetic rats treated with TDF (group DT) (37.50 ± 2.239) compared with DC (51.01 ± 2.205). However, the administration of TDF-AgNPs to diabetic rats significantly improved the SAP (62.39 ± 2.265) compared with DC (51.01 ± 2.205) and diabetic rats treated with TDF only (37.50 ± 2.239). The diabetic rats treated with TDF-AgNPs (group DST) (28.57± 0.7190) had a significant decrease in the percentage of SAR compared to groups DC (37.29 ± 1.554) and DT (38.43 ± 2.181).

TDF-AgNPs alleviates oxidative stress

As presented in Figure 1, there was a significant ($p < 0.05$) increase in MDA but a decrease in GSH, SOD, and CAT in the diabetic group (DC) compared with NC. The diabetic rats treated with TDF (group DT) had no significant difference in GSH, SOD, and CAT compared with DC. However, MDA was significantly increased in group DT (10.71 ± 0.47) compared with the DC (11.94 ± 0.58). Notably, the diabetic rats treated with TDF-AgNPs (group DST) **(**15.04 ± 04**)** had a significant ($p < 0.05$) decrease in MDA level compared with the DC group (11.94 ± 0.58). Also, there was a significant increase in GSH, SOD, and CAT in group DST compared with group DT.

TABLE 2. Y maze parameters (SAP and SAR) for cognitive functions

Groups	Spontaneous alternation	Same arm return
Group 1 (NC)	84.76±1.561	21.43±0.8411
Group 2 (NT)	82.71±2.296	22.86±0.7047
Group 3 (NST)	85.00±1.543	23.14±1.317
Group 4 (DC)	51.01±2.205[a]	37.29±1.554[a]
Group 5 (DT)	37.50±2.239[b]	38.43±2.181
Group 6 (DST)	62.39±2.265[c]	28.57±0.7190[bc]

[a]$p<0.05$ versus NC, [b]$p<0.05$ versus DC, [c]$p<0.05$ versus DT. NC=nondiabetic control, NT=Non-diabetic+TDF, NST=Non-diabetic+silver nanoparticles+TDF, DC=Diabetic control, DT=diabetic+TDF, DST=Diabetic+silver nanoparticles+TDF

TDF-AgNPs reduces PFC IL-1β

As presented in Figure 2, the concentration of IL-1β (an inflammatory marker) was significantly ($p < 0.05$) increased in DC (group DC) (68.550 ± 2.69) compared to NC (group NC) (35.48 ± 1.77). Group DT showed a significant ($p < 0.05$) increase in IL-1β (83.24 ± 2.33) compared with group DC (68.550 ± 2.69). Notably, administration of TDF-AgNPs to diabetic rats showed a significant improvement in IL-1β compared (57.32 ± 1.80) with diabetic rats treated with TDF only (83.24 ± 2.33).

TDF-AgNPs improves GFAP positive astrocytes of the PFC

As shown in (Figure 3A-F), there was a significant ($p < 0.05$) decrease in PFC-GFAP positive astrocytes in DC (20.28 ± 0.55) (DC, Figure 3D) compared with NC (40 ± 2.13) (NC). The diabetic rats treated with TDF only (group DT, Figure 3E) had a significant ($p < 0.05$) reduction in PFC-GFAP positive astrocytes (19 ± 1.52) compared with DC (20.28 ± 0.55) (DC). Interestingly, group DST (Diabetic + TDF-AgNPs) had an improved number of PFC-GFAP positive astrocytes (29.17 ± 0.89) (Figure 3F) compared with group DC and group DT (diabetic + TDF).

## TDF-AgNPs improves ultrastructure of neuronal mitochondrial and glial cells

As shown in (Figure 4A-F), the neuronal mitochondria in group NC (non-diabetes control) appeared normal with a round shape, an intact mitochondrial membrane, and numerous surrounding myelin sheaths (Figure 4A). The non-diabetic rat treated with TDF (group NT) showed an elongated mitochondrion (Figure 4B). Vacuolation and prominent mitochondria were seen in DC (group DC, Figure 4D) compared with group NC. Diabetic rats treated with TDF show few myelin sheaths with disrupted and prominent mitochondria (Figure 4E). Notably, group DST (Diabetes+ TDF-AgNPs) showed round-shaped mitochondria with thick and smooth edges of the myelin sheath (Figure 4F).

TDF-AgNPs preserves PFC pyramidal cells

The effect of TDF and TDF-AgNPs on the PFC pyramidal cells in non-diabetic and diabetic rats is presented in (Figure 5 A-F). The PFC in all non-diabetic groups (Figure 5A-C) shows deep Nissl staining of the pyramidal cells. The DC group (Figure 5D) showed necrotic pyramidal cells and poorly stained Nissl bodies. The diabetic rats treated with TDF only had poor Nissl staining outcomes and scanty pyramidal cells with weak affinity for Nissl stain. Notably, the diabetic rats treated with TDF-AgNPs show improved Nissl staining characteristics of PFC pyramidal cells (Figure 5F).
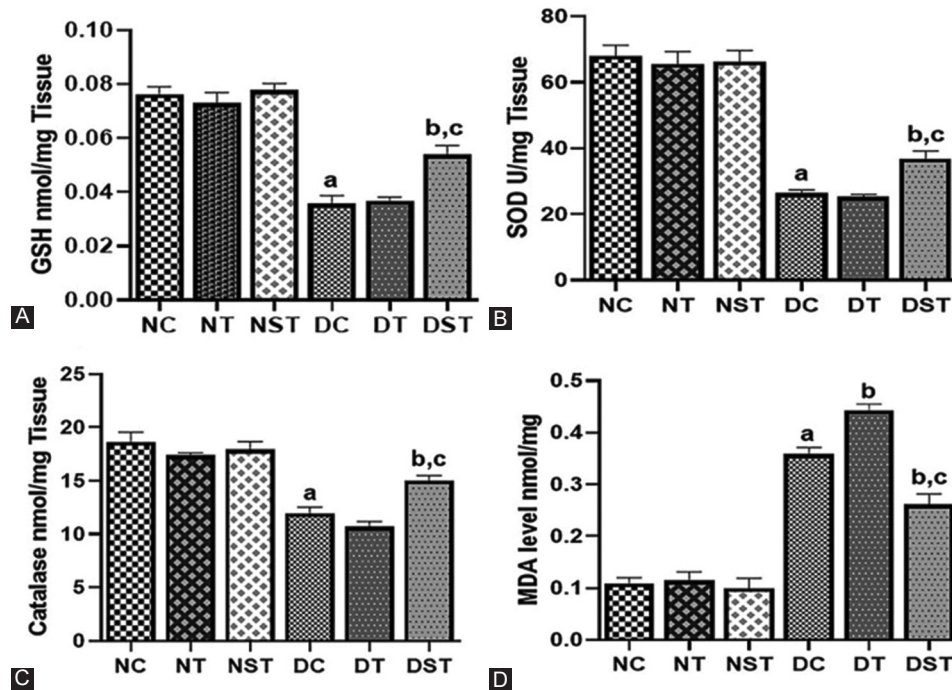
FIGURE 1. Effect of TDF-AgNPs on oxidative stress markers (GSH, SOD, CAT and MDA). (A) p < 0.05 vs NC, (B) p < 0.05 v DC, (C) p < 0.05 v DT. NC=nondiabetic control, NT=non-diabetic + TDF, NST=non-diabetic+ silver nanoparticles + TDF, DC= diabetic control, DT=diabetic + TDF, DST= diabetic +silver nanoparticles+ TDF, A= Reduced glutathione, B= superoxide dismutase (SOD), C = catalase (CAT), Reduced glutathione D= malondialdehyde (MDA).
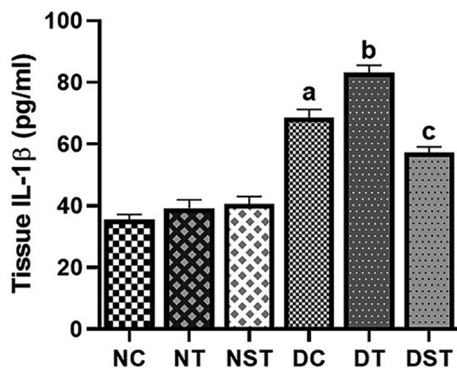

FIGURE 2. Effect of TDF-AgNPs on interleukin-1 beta (IL-1β). ap < 0.05 vs NC, bp < 0.05 v DC, cp < 0.05 v DT. NC=nondiabetic control, NT=non-diabetic + TDF, NST=non-diabetic+ silver nanoparticles + TDF, DC= diabetic control, DT=diabetic + TDF, DST= diabetic +silver nanoparticles+ TDF, interleukin-1 beta (IL-1β).

DISCUSSION

This study evaluated the benefits of tenofovir-silver nanoparticles conjugate on the ultrastructural and cytoarchitectonic properties of the PFC in type-2 diabetic rats. TDF is commonly used as pre-exposure prophylaxis alone or in combination with other antiretroviral drugs as post-exposure prophylaxis [46,47]. Despite TDF's low CNS-penetration rate, studies have reported its neurotoxic effect, diabetic and neurocognitive implications [11,12,19]. Silver nanoparticles have been shown to cross the bloodbrain barrier independent of dosage and route of administration [48,49]. In addition, silver nanoparticles possess antidiabetic and antioxidant effects and long-term drug release ability, which may be suitable for delivering TDF to brain tissues.

This study showed a significant increase in BG in diabetic rats treated with TDF only. Incidences of insulin resistance and hyperglycemia have been reported in the long-term use of NRTIs. Thus, they are associated with type-2 diabetes mellitus [50,51]. However, a study indicated that TDF alone has less risk of insulin resistance [52]. Administration of TDF to diabetic rats in this study caused a significant negative impact on PFC IGF-1. Further decrease in IGF-1 observed in diabetic rats treated with TDF compared with DC rats indicated that TDF exacerbated hyperglycemia in diabetic rats by reducing the IGF-1 level. Previous studies have stated the negative effect of diabetes and TDF on IGF-1 levels in blood and brain samples [16,17]. Notably, TDF-AgNPs treated diabetic rats showed a decrease in BG level that corresponded with a significant improvement in IGF-1. The improvement in glycaemic status and IGF-1 level in diabetic rats treated with TDF-AgNPs may be due to antidiabetic and antioxidant effects of silver nanoparticles in the conjugates via scavenging the free radicals caused by TDF and diabetes [53,54]. In addition, silver nanoparticles have been shown to influence glycaemic control by enhancing hepatic glycogenesis via the insulin signaling pathway and increasing serum insulin concentration [55]. These factors may contribute to the blood-glucose-lowering effects observed in the diabetic rats treated with TDF-AgNPs.
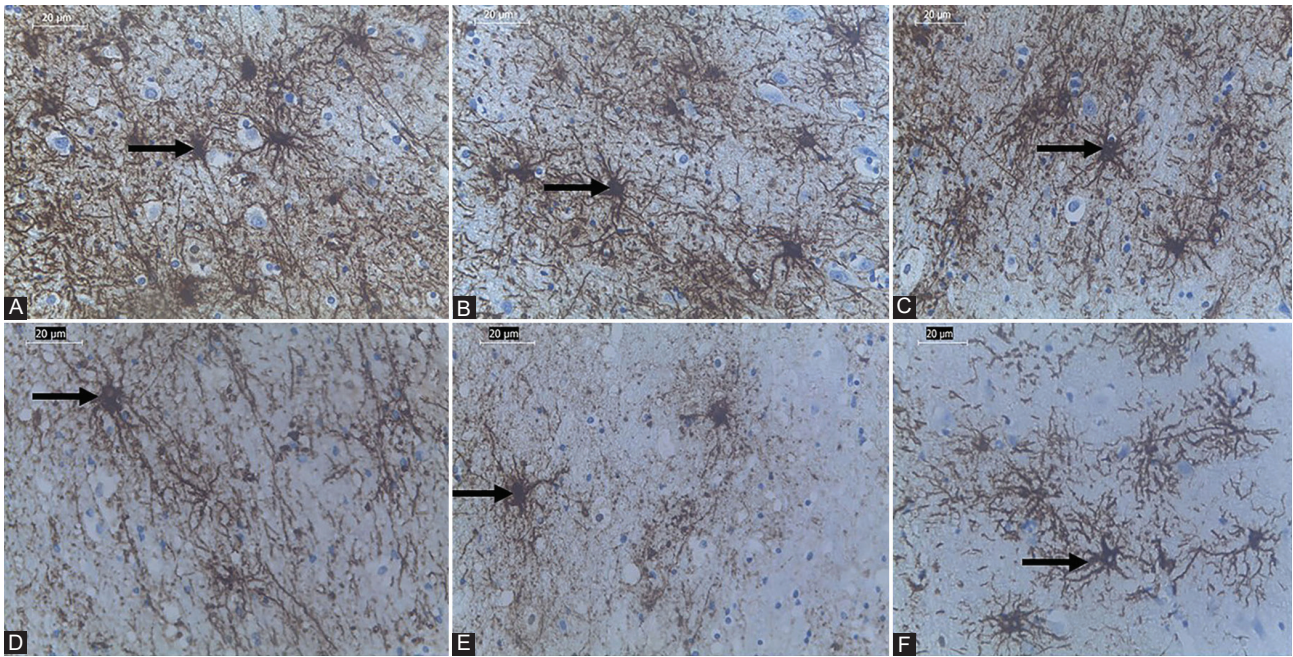
FIGURE 3. Effect of TDF-AgNPs on PFC-GFAP positive astrocytes. (A) nondiabetic control (NC), (B) non-diabetic + TDF (NT), (C) non-diabetic+ silver nanoparticles + TDF (NST), (D) diabetic control (DC), (E) diabetic + TDF (DT), (F) diabetic +silver nanoparticles+ TDF (DST). Black arrow indicates GFAP positive astrocyte.
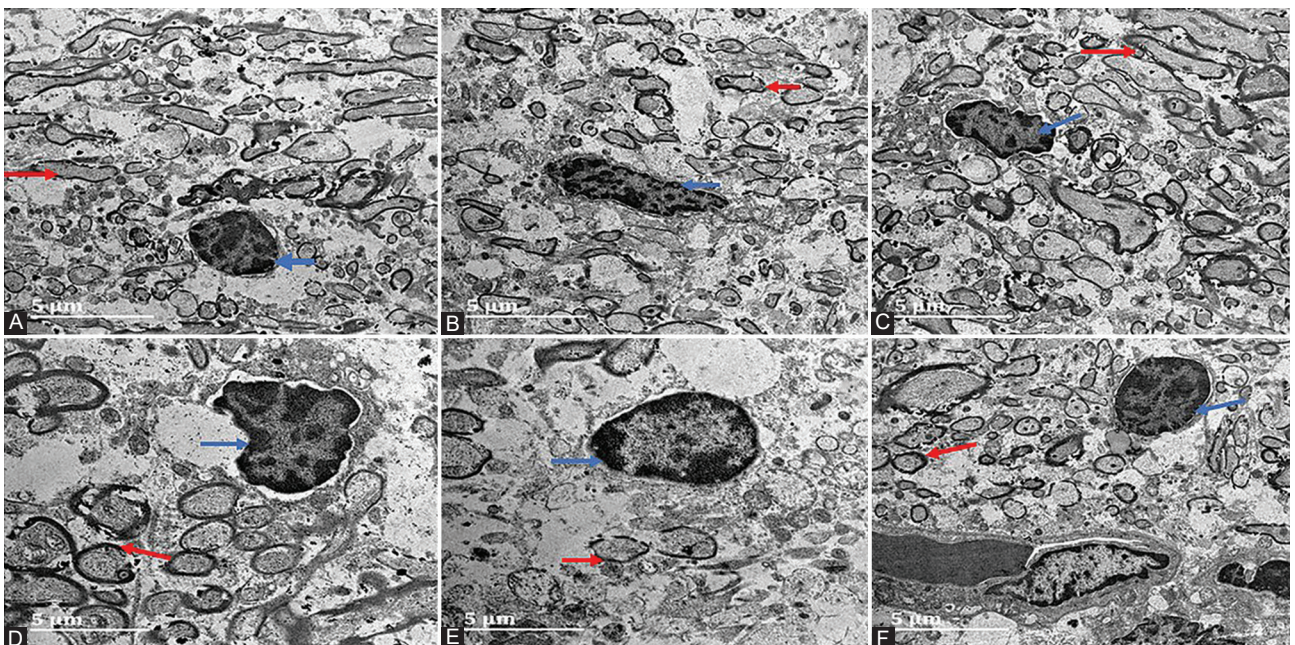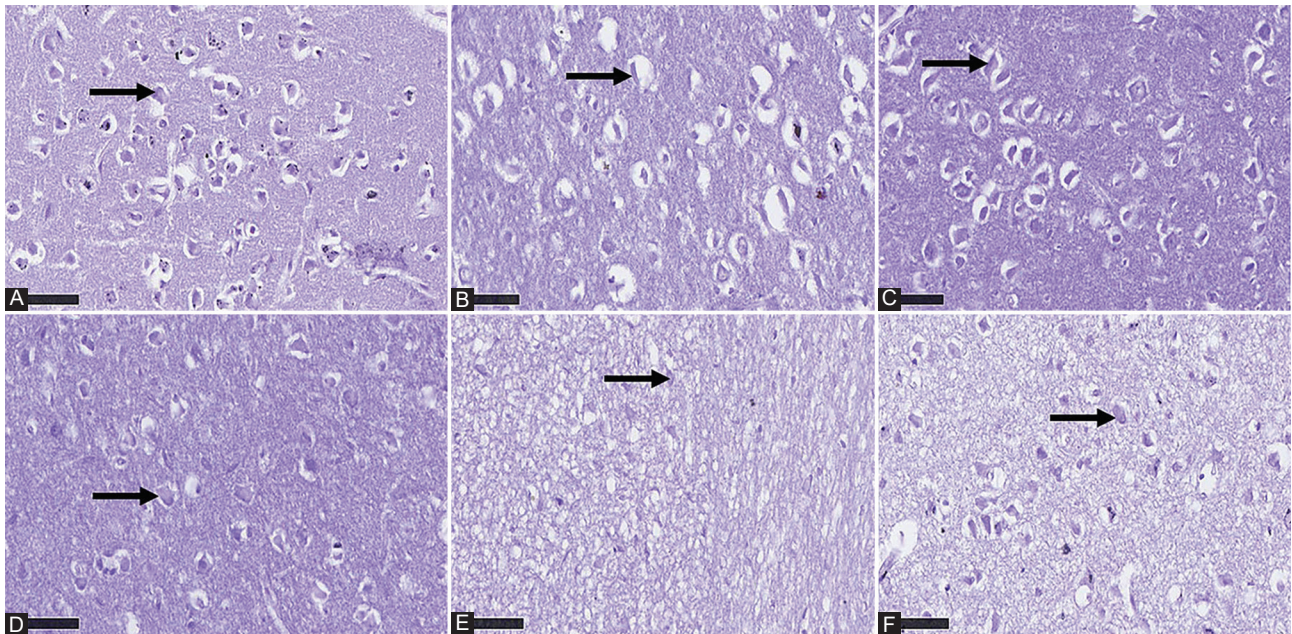

FIGURE 4. Effect of TDF-AgNPs on PFC neuronal mitochondrial and glial cells. (A) nondiabetic control (NC), (B) non-diabetic + TDF (NT), (C) non-diabetic+ silver nanoparticles + TDF (NST), (D) diabetic control (DC), (E) diabetic + TDF (DT), (F) diabetic +silver nanoparticles+ TDF (DST). Blue Arrow indicates neuronal mitochondrial and red arrow indicates glial cells.

Furthermore, MDA significantly increased in diabetic rats treated with TDF only, correlating with hyperglycemia. Chronic hyperglycemia has been linked to increased free radical production and oxidative stress [56]. More so, TDF has been particularly implicated in mitochondrial toxicity [57].

Interestingly, tenofovir-silver nanoparticles conjugate (TDF-AgNPs) alleviated the oxidative stress in the diabetic rats via reducing the MDA while increasing the antioxidant enzymes (GSH, SOD, and CAT). This finding suggests that silver nanoparticles' antioxidant property may alleviate free radical damage caused by diabetes and TDF while promoting the antioxidant enzymes in diabetic rats. Studies have attributed antioxidant properties of AgNPs to inhibition of reactive oxygen species production and improved activities of antioxidant enzymes, thereby scavenging free radicals [53,58].

FIGURE 5. (A-F) Effect of TDF and TDF-AgNPs on the prefrontal cortex pyramidal cells using Nissl staining in non-diabetic and diabetic rats. (A) nondiabetic control (NC), (B) non-diabetic + TDF (NT), (C) non-diabetic + silver nanoparticles + TDF (NST), (D) diabetic control (DC), (E) diabetic + TDF (DT), (F) diabetic + silver nanoparticles + TDF (DST). Black arrow indicates pyramidal cells Nissl stain x 800, 50 μm.

Further investigation on diabetes and TDF treatment showed an increase in the PFC inflammatory cytokine level. An increase in free radical and oxidative injury compromises the integrity of the PFC tissue, which may account for the elevated IL-1β and its neuroinflammatory effects. The diabetic TDF-treated rats had a significant reduction in GFAP positive astrocytes and an increase in mitochondrial damage with few myelin sheaths on ultrastructural assessment. These results corroborate the report of Zulu and colleagues [7], who observed up-regulation of IL-1β, brain tissue injury, and neurocognitive disorder in experimental rats treated with TDF.

The consequences of the PFC tissue damage via oxidative injury and neuroinflammation were obviously seen during the behavioral assessment in this study. TDF caused a decrease in spontaneous alternation performance in diabetic rats while the SAR s significantly increased. This observation indicates a neurocognitive disorder and supports the findings of Zulu *et al.* [7], who reported that TDF promotes neuroinflammation and contributes to the neurocognitive disorder.

In this study, tenofovir-silver nanoparticles (TDF-AgNPs) reduced the neuroinflammatory marker (IL-1β) and preserved the PFC-GFAP positive astrocytes and neuronal organelles. Consequently, these neuroprotective effects were correlated with improved neurobehavioral activities. Oxidative injury and neuroinflammation of PFC tissue are implicated in neurocognitive disorders [59]. Notably, TDF-AgNPs preserved some of the pyramidal cells of the PFC in the diabetic rats compared with the diabetic TDF-treated only rats. An increase in Nissl staining of the pyramidal cells in this group suggested that some of the Nissl bodies were protected by the

antioxidant properties of silver nanoparticles. More so, the overall improvement in the PFC cytoarchitectures was associated with improved cognitive functions.

Silver nanoparticles act as anti-inflammatory and antioxidant agents, protecting the neuronal cell against diabetes and TDF-induced oxidative injury [55,60]. More so, a recent study has reported the advantage of using silver nanoparticles for tissue restoration and regeneration [30,60]. This indicates that an improvement in the neurocognitive functions observed in the tenofovir-silver nanoparticles conjugate treated rats may be attributed to the potency of silver nanoparticles to restore or delay neuronal cell injury. Moreover, TSC used as a reducing and stabilizing agent in the preparation of silver nanoparticles has been reported to influence the toxicity profile by reducing Ag^+ to Ag^o in the conjugates [61,62]. In addition, the size and shape of nanoparticles are determining factors in their biological system interaction and organ toxicity [63]. In this study, the characterization of TDF-AgNPs revealed nanoparticles between 20 and 35 nm with a spherical shape. The observed size and shape may influence the positive impact of silver nanoparticles observed in TDF-AgNPs treated diabetic rats. Previous animal studies showed no adverse effects and organ toxicity in chemically synthesized small-medium silver nanoparticles between 20 nm and 50 nm [64,65].

CONCLUSION

This study suggests that TDF-AgNPs attenuated cognitive deficits via antioxidant and anti-inflammatory properties of silver nanoparticles by preventing the loss of astrocytes and

neurons of the PFC. This drug formulation may be used to ameliorate neurological dysfunction caused by prolonged administration of TDF, HIV-associated neurological disorders, and neglected ART-induced neurological deficits in managing HIV infection.

ACKNOWLEDGMENTS

REFERENCES

[1] Ahmed A, Saqlain M, Bashir N, Dujaili J, Hashmi F, Mazhar F, *et al.* Health-related quality of life and its predictors among adults living with HIV/AIDS and receiving antiretroviral therapy in Pakistan. Qual Life Res 2021;30(6):1653-64.
https://doi.org/10.1007/s11136-021-02771-y

[2] Desta A, Biru TT, Kefale AT. Health related quality of life of people receiving highly active antiretroviral therapy in Southwest Ethiopia. PLoS One 2020;15(8):e0237013.
https://doi.org/10.1371/journal.pone.0237013

[3] Cobucci RN, Lima PH, de Souza PC, Costa VV, Cornetta Mda C, Fernandes JV, et al. Assessing the impact of HAART on the incidence of defining and non-defining AIDS cancers among patients with HIV/AIDS: A systematic review. J Infect Public Health 2015;8(1):1-10.
https://doi.org/10.1016/j.jiph.2014.08.003

[4] World Health Organization. Consolidated Guidelines on the Use of Antiretroviral Drugs for Treating and Preventing HIV Infection: Recommendations for a Public Health approach. Geneva: World Health Organization; 2016.

[5] Eshun-Wilson I, Awotiwon AA, Germann A, Amankwaa SA, Ford N, Schwartz S, et al. Effects of community-based antiretroviral therapy initiation models on HIV treatment outcomes: A systematic review and meta-analysis. PLoS Med 2021;18(5):e1003646.
https://doi.org/10.1371/journal.pmed.1003646

[6] Akang EN. Combination antiretroviral therapy (cART)-induced hippocampal disorders: Highlights on therapeutic potential of Naringenin and Quercetin. IBRO Rep 2019;6:137-46.
https://doi.org/10.1016/j.ibror.2019.04.002

[7] Zulu SS, Abboussi O, Simola N, Mabandla MV, Daniels WM. Effects of combination antiretroviral drugs (cART) on hippocampal neuroplasticity in female mice. J Neurovirol 2021;27(2):325-33.
https://doi.org/10.1007/s13365-021-00967-z

[8] Maartens G, Celum C, Lewin SR. HIV infection: Epidemiology, pathogenesis, treatment, and prevention. Lancet 2014;384(9939):258-71.
https://doi.org/10.1016/S0140-6736(14)60164-1

[9] Waters L, Mehta V, Gogtay J, Boffito M. The evidence for using tenofovir disoproxil fumarate plus lamivudine as a nucleoside analogue backbone for the treatment of HIV. J Virus Erad 2021;7(1):100028.
https://doi.org/10.1016/j.jve.2021.100028

[10] Letendre S, Marquie-Beck J, Capparelli E, Best B, Clifford D, Collier AC, et al. Validation of the CNS penetration-effectiveness rank for quantifying antiretroviral penetration into the central nervous system. Arch Neurol 2008;65(1):65-70.
https://doi.org/10.1001/archneurol.2007.31

[11] Van den Hof M, Blokhuis C, Cohen S, Scherpbier HJ, Wit F, Pistorius MC, et al. CNS penetration of ART in HIV-infected children. J Antimicrob Chemother 2018;73(2):484-9.
https://doi.org/10.1093/jac/dkx396

[12] Mann SC, Morrow M, Coyle RP, Coleman SS, Saderup A,

Zheng JH, et al. Lower cumulative antiretroviral exposure in people living with HIV and diabetes mellitus. J Acquir Immune Defic Syndr 2020;85(4):483-8.
https://doi.org/10.1097/QAI.0000000000002460

[13] Chen YF, Stampley JE, Irving BA, Dugas TR. Chronic nucleoside reverse transcriptase inhibitors disrupt mitochondrial homeostasis and promote premature endothelial senescence. Toxicol Sci 2019;172(2):445-56.
https://doi.org/10.1093/toxsci/kfz203

[14] Wassner C, Bradley N, Lee Y. A review and clinical understanding of tenofovir: tenofovir disoproxil fumarate versus tenofovir alafenamide. J Int Assoc Provid AIDS Care 2020;19:2325958220919231.
https://doi.org/10.1177/2325958220919231

[15] Talia C, Connolly L, Fowler PA. The insulin-like growth factor system: A target for endocrine disruptors? Environ Int 2021;147:106311.
https://doi.org/10.1016/j.envint.2020.106311

[16] Aksu I, Ates M, Baykara B, Kiray M, Sisman AR, Buyuk E, et al. Anxiety correlates to decreased blood and prefrontal cortex IGF-1 levels in streptozotocin induced diabetes. Neurosci Lett 2012;531(2):176-81.
https://doi.org/10.1016/j.neulet.2012.10.045

[17] Erlandson KM, Fiorillo SP, Cardoso SW, Riviere C, Sanchez J, Hakim J, et al. Insulin-like growth factor is associated with changes in body composition with antiretroviral therapy initiation. AIDS Res Hum Retroviruses 2017;33(9):929-34.
https://doi.org/10.1089/AID.2016.0327

[18] Apostolova N, Blas-Garcia A, Esplugues JV. Mitochondrial interference by anti-HIV drugs: mechanisms beyond Pol-gamma inhibition. Trends Pharmacol Sci 2011;32(12):715-25.
https://doi.org/10.1016/j.tips.2011.07.007

[19] Patel PH, Zulfiqar H. Reverse Transcriptase Inhibitors. Treasure Island, FL: StatPearls; 2020.

[20] Rossignol DA, Frye RE. Evidence linking oxidative stress, mitochondrial dysfunction, and inflammation in the brain of individuals with autism. Front Physiol 2014;5:150.
https://doi.org/10.3389/fphys.2014.00150

[21] Picca A, Calvani R, Coelho-Junior HJ, Landi F, Bernabei R, Marzetti E. Mitochondrial dysfunction, oxidative stress, and neuroinflammation: Intertwined roads to neurodegeneration. Antioxidants (Basel) 2020;9(8):647.
https://doi.org/10.3390/antiox9080647

[22] Bizon JL, Foster TC, Alexander GE, Glisky EL. Characterizing cognitive aging of working memory and executive function in animal models. Front Aging Neurosci 2012;4:19.
https://doi.org/10.3389/fnagi.2012.00019

[23] Friedman NP, Robbins TW. The role of prefrontal cortex in cognitive control and executive function. Neuropsychopharmacology 2022;47(1):90-103.
https://doi.org/10.1038/s41386-021-01152-w

[24] Zanto TP, Gazzaley A. Aging of the frontal lobe. Handb Clin Neurol 2019;163:369-89.
https://doi.org/10.1016/B978-0-12-804281-6.00020-3

[25] Pajkrt D, Blokhuis C, Caan M, Kootstra N. Neurodevelopmental Delay in Pediatric HIV/AIDS: Current Perspectives. Neurobehavioral HIV Medicine; 2016.

[26] Naidu EC, Olojede SO, Lawal SK, Rennie CO, Azu OO. Nanoparticle delivery system, highly active antiretroviral therapy, and testicular morphology: The role of stereology. Pharmacol Res Perspect 2021;9(3):e00776.
https://doi.org/10.1002/prp2.776

[27] Lawal SK, Olojede SO, Dare A, Faborode OS, Naidu EC, Rennie CO, et al. Silver nanoparticles conjugate attenuates highly active antiretroviral therapy-induced hippocampal nissl substance and cognitive deficits in diabetic rats. J Diabetes Res 2021;2021:2118538.
https://doi.org/10.1155/2021/2118538

[28] Kumar L, Verma S, Prasad DN, Bhardwaj A, Vaidya B, Jain AK. Nanotechnology: A magic bullet for HIV AIDS treatment. Artif Cells Nanomed Biotechnol 2015;43(2):71-86.

https://doi.org/10.3109/21691401.2014.883400

[29] Marin S, Vlasceanu GM, Tiplea RE, Bucur IR, Lemnaru M, Marin MM, et al. Applications and toxicity of silver nanoparticles: A recent review. Curr Top Med Chem 2015;15(16):1596-604.
https://doi.org/10.2174/1568026615666150414142209

[30] Burdusel AC, Gherasim O, Grumezescu AM, Mogoanta L, Ficai A, Andronescu E. Biomedical applications of silver nanoparticles: An up-to-date overview. Nanomaterials (Basel) 2018;8(9):681.
https://doi.org/10.3390/nano8090681

[31] Gopal J, Abdelhamid HN, Huang JH, Wu HF. Nondestructive detection of the freshness of fruits and vegetables using gold and silver nanoparticle mediated graphene enhanced Raman spectroscopy. Sens Actuators B Chem 2016;224:413-24.
https://doi.org/10.1016/j.snb.2015.08.123

[32] Shastri L, Abdelhamid HN, Nawaz M, Wu HF. Synthesis, characterization and bifunctional applications of bidentate silver nanoparticle assisted single drop microextraction as a highly sensitive preconcentrating probe for protein analysis. RSC Adv 2015;5(52):41595-603.

[33] Everson F, Genis A, Ogundipe T, De Boever P, Goswami N, Lochner A, et al. Treatment with a fixed dose combination antiretroviral therapy drug containing tenofovir, emtricitabine and efavirenz is associated with cardioprotection in high calorie diet-induced obese rats. PLoS One 2018;13(12):e0208537.
https://doi.org/10.1371/journal.pone.0208537

[34] Wilson RD, Islam MS. Fructose-fed streptozotocin-injected rat: An alternative model for Type 2 diabetes. Pharmacol Rep 2012;64(1):129-39.
https://doi.org/10.1016/s1734-1140(12)70739-9

[35] Nocito L, Zafra D, Calbo J, Dominguez J, Guinovart JJ. Tungstate reduces the expression of gluconeogenic enzymes in STZ rats. PLoS One 2012;7(8):e42305.
https://doi.org/10.1371/journal.pone.0042305

[36] Turkevich J, Stevenson P, Hillier J. The size and shape factor in colloidal systems. ??? 1951;11:55.

[37] Govender S, Lutchman D, Pillay V, Chetty DJ, Govender T. Enhancing drug incorporation into tetracycline-loaded chitosan microspheres for periodontal therapy. J Microencapsul 2006;23(7):750-61.
https://doi.org/10.1080/02652040600789229

[38] Hughes RN. The value of spontaneous alternation behavior (SAB) as a test of retention in pharmacological investigations of memory. Neurosci Biobehav Rev 2004;28(5):497-505.
https://doi.org/10.1016/j.neubiorev.2004.06.006

[39] Typlt M, Mirkowski M, Azzopardi E, Ruettiger L, Ruth P, Schmid S. Mice with deficient BK channel function show impaired prepulse inhibition and spatial learning, but normal working and spatial reference memory. PLoS One 2013;8(11):e81270.
https://doi.org/10.1371/journal.pone.0081270

[40] Kakkar P, Das B, Viswanathan PN. A modified spectrophotometric assay of superoxide dismutase. Indian J Biochem Biophys 1984;21(2):130-2.

[41] Aebi H. Catalase. In: Methods of Enzymatic Analysis. Amsterdam, Netherlands: Elsevier; 1974. p. 673-84.

[42] Ellman GL. Tissue sulfhydryl groups. Arch Biochem Biophys 1959;82(1):70-7.
https://doi.org/10.1016/0003-9861(59)90090-6

[43] Mkhwanazi BN, Serumula MR, Myburg RB, Van Heerden FR, Musabayane CT. Antioxidant effects of maslinic acid in livers, hearts and kidneys of streptozotocin-induced diabetic rats: Effects on kidney function. Ren Fail 2014;36(3):419-31.
https://doi.org/10.3109/0886022X.2013.867799

[44] Gu JX, Cheng XJ, Luo X, Yang X, Pang YP, Zhang XF, et al. Luteolin ameliorates cognitive impairments by suppressing the expression of inflammatory cytokines and enhancing synapse-associated proteins GAP-43 and SYN levels in streptozotocin-induced diabetic rats. Neurochem Res 2018;43(10):1905-13.
https://doi.org/10.1007/s11064-018-2608-6

[45] Djidja MC, Claude E, Scriven P, Allen DW, Carolan VA, Clench MR. Antigen retrieval prior to on-tissue digestion of formalin-fixed paraffin-embedded tumour tissue sections yields oxidation of proline residues. Biochim Biophys Acta Proteins Proteom 2017;1865(7):901-6.
https://doi.org/10.1016/j.bbapap.2016.11.019

[46] Bekker LG, Brown B, Joseph-Davey D, Gill K, Moorhouse M, Delany-Moretlwe S, et al. Southern African guidelines on the safe, easy and effective use of pre-exposure prophylaxis: 2020. South Afr J HIV Med 2020;21(1):1152.
https://doi.org/10.4102/sajhivmed.v21i1.1152

[47] Chauveau M, Billaud E, Bonnet B, Merrien D, Hitoto H, Bouchez S, et al. Tenofovir DF/emtricitabine/rilpivirine as HIV post-exposure prophylaxis: Results from a multicentre prospective study. J Antimicrob Chemother 2019;74(4):1021-7.
https://doi.org/10.1093/jac/dky547

[48] Greish K, Alqahtani AA, Alotaibi AF, Abdulla AM, Bukelly AT, Alsobyani FM, et al. The effect of silver nanoparticles on learning, memory and social interaction in BALB/C mice. Int J Environ Res Public Health. 2019;16(1):148.
https://doi.org/10.3390/ijerph16010148

[49] Struzynska L, Skalska J. Mechanisms underlying neurotoxicity of silver nanoparticles. Adv Exp Med Biol 2018;1048:227-50.
https://doi.org/10.1007/978-3-319-72041-8_14

[50] Dagogo-Jack S. HIV therapy and diabetes risk. Diabetes Care 2008;31(6):1267-8.
https://doi.org/10.2337/dc08-0459

[51] Garcia-Benayas T, Rendon AL, Rodriguez-Novoa S, Barrios A, Maida I, Blanco F, et al. Higher risk of hyperglycemia in HIV-infected patients treated with didanosine plus tenofovir. AIDS Res Hum Retroviruses 2006;22(4):333-7.
https://doi.org/10.1089/aid.2006.22.333

[52] Randell PA, Jackson AG, Zhong L, Yale K, Moyle GJ. The effect of tenofovir disoproxil fumarate on whole-body insulin sensitivity, lipids and adipokines in healthy volunteers. Antivir Ther 2010;15(2):227-33.
https://doi.org/10.3851/IMP1518

[53] Chandrasekhar N, Vinay SP. Yellow colored blooms of Argemone mexicana and Turnera ulmifolia mediated synthesis of silver nanoparticles and study of their antibacterial and antioxidant activity. Appl Nanosci 2017;7(8):851-61.
https://doi.org/10.1007/s13204-017-0624-5

[54] Das G, Patra JK, Debnath T, Ansari A, Shin HS. Investigation of antioxidant, antibacterial, antidiabetic, and cytotoxicity potential of silver nanoparticles synthesized using the outer peel extract of *Ananas comosus* (L.). PLoS One 2019;14(8):e0220950.
https://doi.org/10.1371/journal.pone.0220950

[55] Alkaladi A, Abdelazim AM, Afifi M. Antidiabetic activity of zinc oxide and silver nanoparticles on streptozotocin-induced diabetic rats. Int J Mol Sci 2014;15(2):2015-23.
https://doi.org/10.3390/ijms15022015

[56] Yaribeygi H, Atkin SL, Sahebkar A. A review of the molecular mechanisms of hyperglycemia-induced free radical generation leading to oxidative stress. J Cell Physiol 2019;234(2):1300-12.
https://doi.org/10.1002/jcp.27164

[57] Ramamoorthy H, Abraham P, Isaac B, Selvakumar D. Mitochondrial pathway of apoptosis and necrosis contribute to tenofovir disoproxil fumarate-induced renal damage in rats. Hum Exp Toxicol 2019;38(3):288-302.
https://doi.org/10.1177/0960327118802619

[58] Negahdary M, Chelongar R, Zadeh SK, Ajdary M. The antioxidant effects of silver, gold, and zinc oxide nanoparticles on male mice in *in vivo* condition. Adv Biomed Res 2015;4:69.
https://doi.org/10.4103/2277-9175.153893

[59] de Munter J, Pavlov D, Gorlova A, Sicker M, Proshin A, Kalueff AV, et al. Increased oxidative stress in the prefrontal cortex as a shared feature of depressive and PTSD-like syndromes: Effects of a standardized herbal antioxidant. Front Nutr 2021;8:661455.
https://doi.org/10.3389/fnut.2021.661455

[60] Seethalakshmi AM. Evaluation of *in-vitro* anti-inflammatory

activity of silver nanoparticles synthesised using *Piper nigrum* extract. J Nanomed Nanotechnol 2015;6:2.
https://doi.org/10.4172/2157-7439.1000268

[61] Doddagoudar SR, Sreenivas AG, Ramappa KT, Nidoni U, Hiregoudar S, Yerragopu PS. Chemical synthesis of silver nanoparticles using tri-sodium citrate, stability study and their characterization. Int Res J Pure Appl Chem 2020;21(3):37-50.
https://doi.org/10.9734/irjpac/2020/v21i330159

[62] Shumbula P, Harris R, Nyembe S, Keter FK, Sikhwivhilu L, Tshikhudo R. Cytotoxicity effects of citrate, glucose and cetyltrimethyl ammonium chloride-capped silver nanoparticles in lung epithelial carcinoma cells (A549). Mater Today 2015;2(7):4118-24.
https://doi.org/10.1016/j.matpr.2015.08.042

[63] Ajdary M, Moosavi MA, Rahmati M, Falahati M, Mahboubi M, Mandegary A, et al. Health concerns of various nanoparticles: A review of their *in vitro* and *in vivo* toxicity. Nanomaterials (Basel) 2018;8(9):634.
https://doi.org/10.3390/nano8090634

[64] Lara HH, Ayala-Nunez NV, Ixtepan-Turrent L, Rodriguez-Padilla C. Mode of antiviral action of silver nanoparticles against HIV-1. J Nanobiotechnology 2010;8:1.
https://doi.org/10.1186/1477-3155-8-1

[65] Recordati C, De Maglie M, Bianchessi S, Argentiere S, Cella C, Mattiello S, et al. Tissue distribution and acute toxicity of silver after single intravenous administration in mice: Nano-specific and size-dependent effects. Part Fibre Toxicol 2016;13:12.
https://doi.org/10.1186/s12989-016-0124-x

Related articles published in BJBMS

1. Histological and biochemical effects of Cinnamomum cassia nanoparticles in kidneys of diabetic Sprague-Dawley rats

   Koffi Kouame et al., BJBMS, 2019

2. Different dose-dependent effects of ebselen in sciatic nerve ischemia-reperfusion injury in rats

   Filiz Ozyigit et al., BJBMS, 2015